PREPARATION OF CONDUCTIVE AND FLAME-RETARDANT PU/GO/DOPO PRINTED FILMS

Aslı Beyler Çiğil [1, 2] iD *, Hatice Birtane [2]* iD *, Okan Esentürk [3]* iD
*[1]Amasya University, Department of Chemistry and Chemical Process Technology,
Amasya, Turkey*
[2]Marmara University, Department of Chemistry, Istanbul, Turkey
[3] Middle East Technical University, Department of Chemistry, Ankara, Turkey

Abstract: *Printed electronics are emerging technology products that we use in every moment of our daily lives. It is used in many fields from health, textile, electronics to communication. Inks with nanometal or organic content can be used in printed electronics. The ability of printed electronics to withstand temperature makes its use widespread in the electronics industry. Main aim of the study is to combine surface modified graphene oxide-based conductive inks with flame retardant materials.*
In this study, an effective and simple approach for the preparation of polyurethane acrylate (PUA) screen printing ink containing surface modified reduced graphene oxide (rGO) which has flame retardant activity. A new and effective flame-retardant additive; 9,10-dihydro-9,10-oxa-10-phosphaphenanthrene-10-oxide (DOPO), silane coupling agent and reduced graphene oxide was synthesized. In this synthesis, first reduced graphene oxide was modified with (methacryloyloxy)propyltrimethoxysilane, and then reacted with DOPO to obtain a flame-retardant monomer containing P and Si. Based on the successful modification reactions, screen-printing ink containing polyurethane acrylate and different amounts of modified graphene oxide content (0, 5 and 10 wt%) were prepared and screen printed on the paper surface. In addition, coatings were made on the paper surface to determine some the properties. LOI values, thermal properties, contact angle values, conductivity and surface properties of the obtained prints and coatings films were investigated. As a result, conductive screen-printing ink resistant to high temperatures was successfully produced and printed coatings and free films were formed.

Key words: reduced graphene oxide, polyurethane acrylate coating, UV curable coating, flame retardant, printed electronics

1. INTRODUCTION

Printed electronics have the potential to produce flexible, low-cost electronic devices and systems to realize new applications such as wearables, portable electronics, wireless communications, healthcare, sensors (Gengenbach et al., 2020; Saengchairat et al., 2016; Hines et al., 2021). The most important component of printed electronics are functional inks based on nanomaterials. The ink portfolio is constantly evolving from materials of print conductors, passive components (e.g., capacitors, resistors) and active components (e.g., transistors, diodes) (Garlapati et al., 2018; Wu., 2017). The formulation of high-performance functional inks is a key factor in achieving these goals and demonstrates enormous potential to produce printed electronics (Hong et al., 2022; Zhang et al., 2020; Cronin et al., 2018). Recently, in numerous commercial products and literature, nano-silver particles/flakes, graphene, single-walled carbon nanotubes, organic/oxide semiconductors and conductive polymers is used to prepare conductive inks (Liang et al., 2016; Hyun et al., 2015; Kell et al., 2017; Cao et al., 2018; Chiolerio et al., 2015). The large surface areas of the nanoparticles allow for greater contact area, which contributes to higher conductivity and stability (Faddoul et al., 2012). Moreover, the nanoparticles showed good compatibility with various base polymer resins. Recently, two-dimensional (2D) nanomaterials such as graphene, MXenes and boron nitride (BN) have been extensively investigated due to their good electrical or thermal conductive properties (Sreenilayam et al., 2021; He et al., 2019; Joseph et al., 2016). For example, graphene, one of the inorganic carbon nanomaterials, is one of the fillers used to increase the thermal conductivity of the polymeric matrix with an electrical conductivity of 6000 S cm^{-1} and a high thermal conductivity of 5000 W m^{-1} K^{-1} (Burk et al., 2018).

Important printing techniques such as screen printing, offset printing or inkjet printing have been adapted for the use of functional printing inks (Cronin et al., 2018). Apart from these printing techniques, new printing techniques such as aerosol-jet printing and electrohydrodynamic ink-jet printing have been developed for functional printing applications (Verboven & Deferme, 2021). After the ink is deposited

onto the substrate by the printing process, one or more processing steps such as curing, drying, and sintering are required to obtain the desired functional layer. Most of the previous research and commercial products show the necessity of a high temperature curing process to achieve high electrical conductivity (Htwe & Mariatti, 2022). This high temperature curing process (above approximately 160 °C) after screen printing inevitably causes shrinkage/deformation and strength reduction in most electronic systems. Although alternative techniques such as direct current sintering (DCS), microwave flash sintering, and laser have been reported to successfully achieve high electrical conductivity at low temperature, the complexity of processing, the requirement for expensive equipment, and limited volume manufacturing limit their practical use (Cronin et al., 2018; Perelaer et al., 2009). Recently, UV-curable conductive inks are a potential solution for substrates with low temperature resistance.

UV-initiated radical polymerization has made significant progress in recent years. This is predominantly due to the fast-curing speed at a relatively low temperature with low emissions of volatile organic compounds, which allows printed flexible electronics prepared by UV curing to be more environmentally friendly and more attractive (Mendes-Felipe et al., 2019). Conductive inks prepared from UV-curable prepolymers, and monomers are used to produce printed electrolytes due to their fast UV curing rates, energy efficiency and high dimensional stability (Saleh et al., 2017). However, two major challenges remain for the currently available UV-curable conductive ink. The first challenge comes from the compatibility between UV-curable resins and conductive fillers, as well as the optimization of conductive filler distribution. On the other hand, due to the trade-off between mechanical strength and electrical properties, increasing the conductive filler content to achieve higher electrical conductivity will increase the hardness of the printed electronics, thereby reducing flexibility. Therefore, it is critical to conduct studies on UV-curable conductive ink in different compositions and ratios to produce high-performance printed electronics.

Today, natural, and synthetic polymeric materials are widely used in different fields such as coating, electronics, and cable due to their superior properties such as low density, resistance to erosion and ease of processing (Song et al., 2009; Kashiwagi et al., 2005). These polymeric materials are inherently flammable. However, the fire hazards associated with the use of flammable polymeric materials, which cause great loss of life and property, limit their use in some areas. For this reason, increasing the flame retardancy of polymeric materials becomes a more important and necessary issue for the protection of the environment and human health. For environmental concerns, halogen-free flame-retardant materials have received great attention because halogen-containing flame-retardant materials can produce a lot of smoke and toxic gases during the combustion process (Liu et al., 2010; Chen et al., 2014).

In this study, a new UV-curable conductive ink was prepared and then applied to the paper surface by screen-printing technology on the other hand, these inks are coated on paper as varnish. Silane modification has been used as a surface treatment for the functionalization of reduced graphene oxide (rGO). Acrylate modified rGO was prepared using silanization of rGO with 3-(Trimethoxysilyl)propyl acrylate. A novel flame-retardant additive, DOPO/acrylate modified rGO is synthesized and characterized. The thermal behaviors and flame retardances of the ink/coatings are investigated and found to be influence by the structural features of the m-rGO nanoarticles used. Moreover, contact angle values, surface properties and conductivity of the obtained ink/coatings were investigated.

2. METHODS

2.1 Materials

Reduced graphene oxide (rGO) was obtained from the company Nanography (Turkey). 3-(Trimethoxysilyl)propyl acrylate and trimethylolpropane triacrylate (TMPTA) were obtained from Sigma-Aldrich. 9,10-dihydro-9-oxa-10-phosphaphenanthrene-10-oxide (DOPO) was obtained as a gift from MCTCHEM (Turkey). 2-hydroxy-2-methyl-1-phenyl-1-propanone (Darocur 1173) were obtained from Ciba Specialty Chemicals. Polyurethane acrylate was obtained from Sartomer (CN9782).

2.2 Modification of reduced graphene oxide

0.3 g of rGO was dispersed in 270 ml of ethyl alcohol through ultrasonication for 1 h; 6 g of 3-(Trimethoxysilyl)propyl acrylate was added and the mixture was stirred vigorously at a temperature of 78 °C for 18 h. The mixture was filtered and washed several times with deionized water and ethyl alcohol. Finally, acrylate-modified rGO (acr-rGO) was obtained after vacuum drying at 50 °C for 12 h. Structural characterization were performed with the FTIR. The scheme of the modification is given in Figure 1.
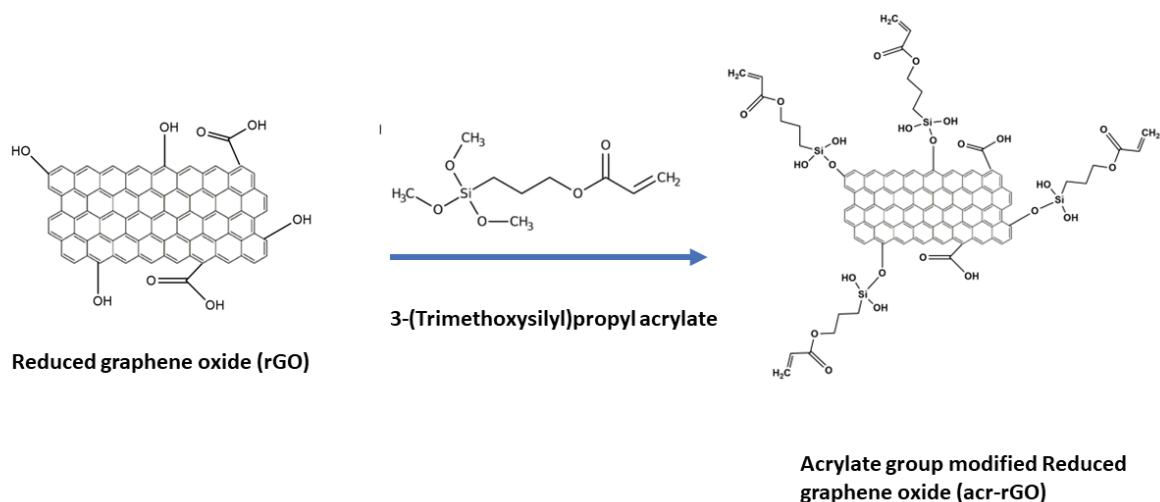
Figure 1: Schematic illustration of the acrylate modification of rGO

The obtained acrylate functional rGO nanoparticles, DOPO (2 g) and Xylene (50 mL) were added into a round bottom flask equipped with magnetic stirring. The reaction was performed for 5 h at 125-130 °C under arc N_2 atmosphere. The mixture was filtered and washed several times with deionized water and ethyl alcohol. Finally, DOPO modified acr-rGO (m-rGO) was obtained after vacuum drying at 40 °C for 12 h. Structural characterization were performed with the FTIR. The scheme of the reaction is given in Figure 2.
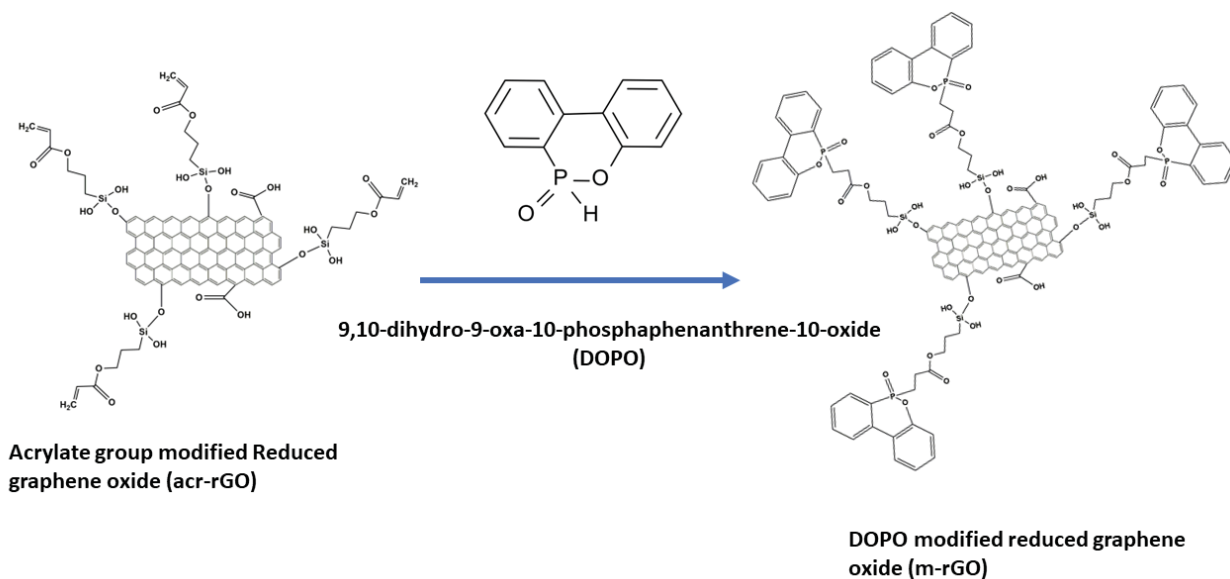

Figure 2: Schematic illustration of the DOPO modification of acr-rGO

2.3 Preparation of UV-curing conductive ink and coating formulations

Four components were used to produce UV-curable conductive ink: conductive filler (surface modified reduced graphene oxide), polymer (polyurethane acrylate), photoinitiator (Darocur 1173), and diluent (TMPTA). The polymer provides ink formation for printing conductive patterns and contributes to the dispersion stability of conductive particles.

In this study, reduced graphene oxide nanoparticles were chosen as the conductive materials. The large surface contact areas between the reduced graphene oxide nanoparticles produce high electrical conductivity and a low permeation threshold. Preferred for improved fill distribution for higher print quality and resolution. PUA as a polymer was chosen to support the flexibility and softness of the printed conductive layers after curing. TMPTA was used as diluents to reduce the viscosity of conductive inks, they can improve the ink penetration through the screen mesh and ink transfer during the screen-

printing process. Darocur 1173 was chosen as the photoinitiator capable of generating reactive species (i.e. free radicals) and initiating chain growth of acrylates when exposed to UV light.

First, three different UV-curing formulations for conductive ink/coating were prepared according to the weight ratios given in Table 1 by mixing PUA, TMPTA, Darocur 1173, m-rGO. Each formulation was taken into a 10 mL beaker and surrounded by aluminum foil. It was kept in an ultrasonic bath until a transparent and homogeneous mixture was obtained. The homogeneous mixtures were degassed in a vacuum oven. The prepared resin was applied to the paper surface by screen-printing method and exposed to 3 minutes UV rays (printed coatings). In addition, coated films were prepared from the obtained formulations for LOI and TGA analyses.

Table 1: UV-curing conductive ink formulation

Ingredients (g)	F0m-rGO	F5m-rGO	F10m-rGO
PUA	3	3	3
TMPTA	2	2	2
m-rGO	-	0,25	0,5
Darocur 1173	0,15	0,15	0,15

2.4 Characterization

Fourier-Transform Infrared Spectroscopy (FTIR) spectra were recorded on a Bruker IFS 66/S spectrometer with ATR capability. Thermal gravimetric analysis (TGA) was carried out by using the Perkin Elmer Instrument STA6000 instrument. The TGA measurements were performed between 30 °C and 750 °C (under N_2, rate 10 °C/min). The limit oxygen index (LOI) values of the coatings were measured by using a FTT (Fire Testing Technology) type instrument, according to ASTM D2863. The test specimen bars of $120 \times 6 \times 3$ mm^3 were prepared for the LOI test. The colours of the obtained coatings were measured by X-Rite eXact portable spectrophotometer according to the ISO 13655:2017 standard. The measurement conditions of the spectrophotometer were determined as polarization filter with 0/45° geometry with 2° observer angle and D50 light source in the range of 400-700 nm. Colour differences were calculated according to the CIELab (2000) technique. ISO 11664-6:2014. Calculations were performed by calculating the average of five measurements. Δ_L*, Δ_a*, and Δ_b*: Difference in L*, a*, and b* values between the specimen and target colours, respectively. The lightness is represented by the L* axis, which ranges from white to black. The red area is connected to green by the a* axis, whereas the b* axis runs from yellow to blue.

$$\Delta E_{00} = \sqrt{\left(\frac{\Delta L'}{k_L S_L}\right)^2 + \left(\frac{\Delta C'}{k_C S_C}\right)^2 + \left(\frac{\Delta H'}{k_H S_H}\right)^2 + R_T \frac{\Delta C'}{k_C S_C} \frac{\Delta H'}{k_H S_H}}$$

(1)

where ΔL*, ΔC*, and ΔH* are the CIEL*a*b* metric lightness, chroma, and hue differences, respectively, calculated between the standard and sample in a pair, and ΔR is the interaction term between the chroma and hue differences. S_L, S_C, and S_H are the weighting functions for lightness, chroma, and hue components, respectively. The values calculated for these functions vary according to the positions of the sample pair considered in the CIEL*a*b* colour space. The k_L, k_C, and k_H values are the parametric factors to be adjusted according to different viewing parameters such as textures, backgrounds, and separations, for the lightness, chroma, and hue components, respectively.

The gloss measurements of all coatings were carried out with the BYK Gardner GmbH micro gloss 75° geometry in accordance with ISO 8254-1:2009. The contact angles of coatings were found on Pocket Goniometer Model PG-X, version 3.4 (FIBRO Systems AB, Sweden). Surface-free energy was calculated according to ASTM D5946 standard test method, depending on the water contact angle. The images of droplets were then recorded by using a CCD video camera. Conductivity was calculated with the formula given below. Voltage and current values were measured with Fluke 179 True RMS Digital Multimeter.

$V=IR$ (2)

$R=\rho l/A$ (3)

4. DISCUSSION

4.1 Structural characterization of surface modified reduced graphene oxide

Surface modified reduced graphene oxides (m-rGO) were structurally characterized by FTIR spectroscopy and the spectra are given in Figure 3. As shown in Figure 3, compared with the spectrum of rGO, the newly formed absorption bands around 2886 cm^{-1} mean that the C–H stretching in aliphatic CH$_2$ groups. More clear evidence for the successful acrylate group modification can be confirmed by strong stretching vibrations for Si–O–C at 1112 and 692 cm^{-1} as well as the stretching and bending vibrations of Si–O at 1056 cm^{-1}, respectively (Huang et al., 2018). Compared with the spectrum of DOPO, the characteristic peak of P-H (in DOPO/acr-rGO) disappeared at 2385 cm^{-1}. By comparison with the spectrum of acr-rGO, the characteristic peak of C=C (in DOPO/Acr-rGO) disappeared at 1623 cm^{-1}. Several new characteristic peaks were observed: 913 cm^{-1} (P-O-phenyl), 1245 cm^{-1} (P=O), 1429 cm^{-1} (P-phenyl), 1581 cm^{-1} (phenyl), 1595 cm^{-1} and 1608 cm^{-1} (Ma et al., 2018; Lin et al., 2020). From the FTIR analysis, it was evident that m-rGO was successfully synthesized.
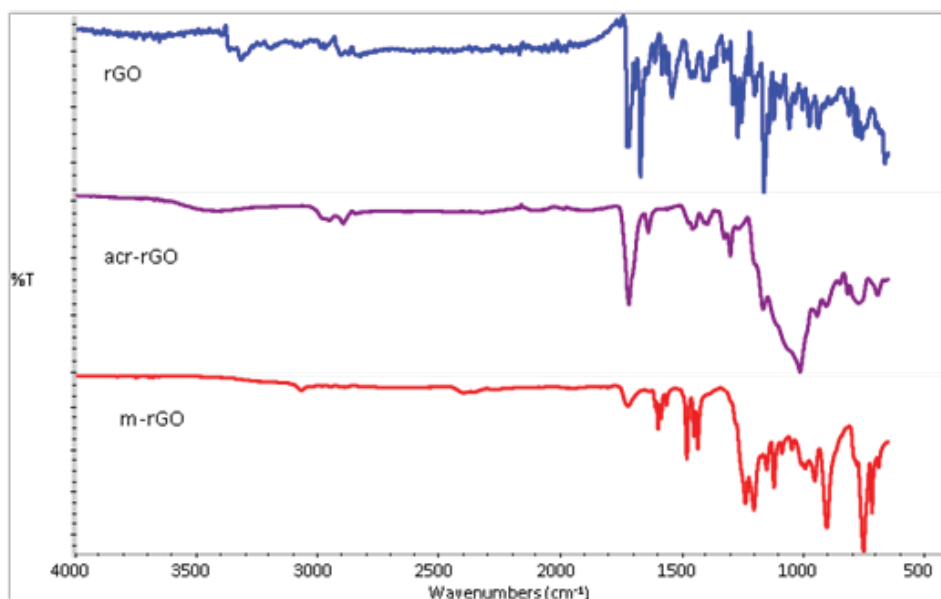

Figure 3: FTIR spectra of the surface modified reduced graphene oxide

4.2 Thermal properties and flame retardancy of the photocured free films

To examine the thermal properties only in terms of polymeric materials, free films were produced. The thermal degradation profiles of the photocured free films were determined TGA. The TGA spectra is presented in Figure 4. The results of the TGA are also collected in Table 2.

Table 2: Thermal properties of the free films

	T$_{max}$[a] (°C)	Char (%)	LOI
F0m-rGO	388,13	0,681	18,5
F5m-rGO	404,61	3,594	20
F10m-rGO	407,21	5,309	20,5

[a] The maximum weight loss temperatures, which were determined from the maximum of the corresponding derivative curves.

Mainly, the free films exhibited a one-step degradation process. The maximum decomposition stages were around 400 °C and this weight loss was attributed to the decomposition of aromatic groups. It was observed that as the amount of m-rGO increased in the formulations, the thermal strength increased slightly.
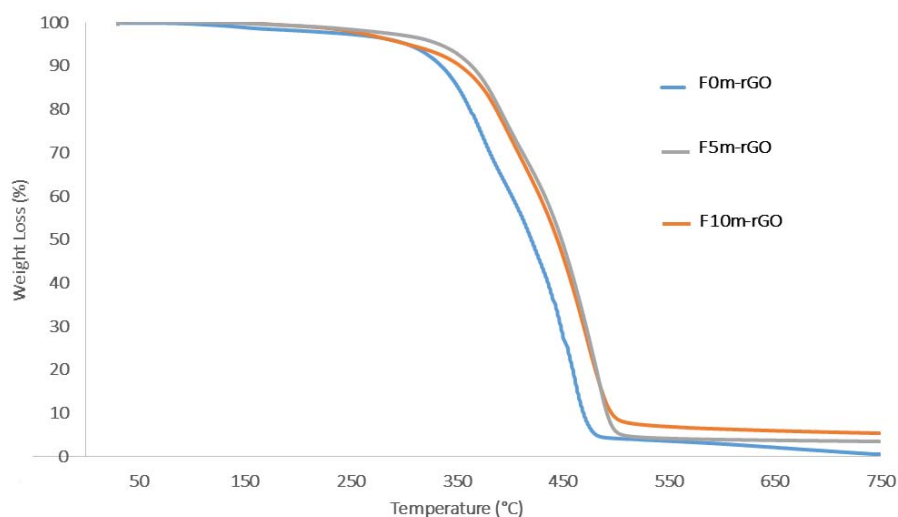
Figure 4: TGA thermograms of the free films

The char yields increased gradually with the increasing amount of m-rGO. When 10 wt% m-rGO nanoparticles are added, the amount of char yields increased from 0,681 to 5,309. The amount of char yields is generally associated with the flame retardancy of materials. Thus, it can be said that the flame retardancy of the m-rGO nanoparticles-containing free films and conductive inks were improved. We further evaluated the flame retardancy of the free films by the LOI test in which the minimum amount of oxygen that is needed to support flaming combustion is measured.

The LOI values of the free films are given in Table 2. The F0m-rGO encoded free film had a LOI value of 18,5. As m-rGO nanoparticles was increased in the free films, the LOI values increased slightly. It is thought that this is because a small amount of DOPO modified reduced graphene oxide (5 and 10% wt) is added to the formulations. The amount of P in the nanoparticles whose surface is modified with DOPO is quite low.

4.3 Printability of coatings

The colour and gloss properties of the obtained coatings were measured and given in Table 3. When the Table 3 was examined, it was seen that the colour of the base paper changed completely with all coatings. In F0m-rGO coatings, which do not contain m-rGO nanoparticles, the colour shifted slightly towards yellow. This is a feature that polyurethane acrylate brings to the coating and is compatible with the literature (Liu & Liu, 2018). It was observed that the coatings added with m-rGO nanoparticles caused a great change in the L value. On visual inspection, the colour of these coatings is black. With the Delta E difference, it is proved that the colour is completely different. As the number of m-rGO nanoparticles increased, the colour difference increased and the colour became darker. Similar results are in the same direction in the literature (Cao & Wang, 2017).

Table 3: Colour and gloss characteristics of coatings

	L	a	b	ΔE_{00}	Gloss
Base paper	100.00	0.02	0.01	-	6.3
F0m-rGO	93.11	-0.21	5.04	4.7	13.4
F5m-rGO	38.68	-0.37	5.55	48.1	11.1
F10m-rGO	29.66	-0.45	6.00	58.2	10.7

When the gloss results were examined, it was determined that the gloss of the coatings was higher than the uncoated paper because the gaps on the surface were filled with the coatings. In the coatings to which m-rGO nanoparticles were added, a small amount of roughness was created, and the gloss decreased a little. This decrease varies depending on the m-rGO nanoparticles ratio. Results are similar to literature (Arman-Kandırmaz et al., 2020).

4.4 Contact angle and Surface energies of coatings

For an ink to adhere to a substrate, there must be a harmony between the surface and the ink, the surface energy, and the contact angle. For this reason, the contact angle of the obtained coatings was measured and given in Figure 5. When examined, the highest contact angle was obtained in the coating without m-rGO nanoparticles. The addition of m-rGO nanoparticles reduced the contact angle. As the number of m-rGO nanoparticles added increased, the decrease in the contact angle increased. The results obtained are compatible with the literature (Tissera et al., 2015). This shows that the interest of the coated substrate has increased against water-based ink. Surface energies were calculated using the obtained contact angles. Surface energies of F0m-rGO, F5m-rGO, F10m-rGO coatings were determined as 40.8, 46.6, 47 (mJ/m^2) respectively. The surface energy increased as the contact angle decreased. These are the expected results (Ozcan et al., 2020).
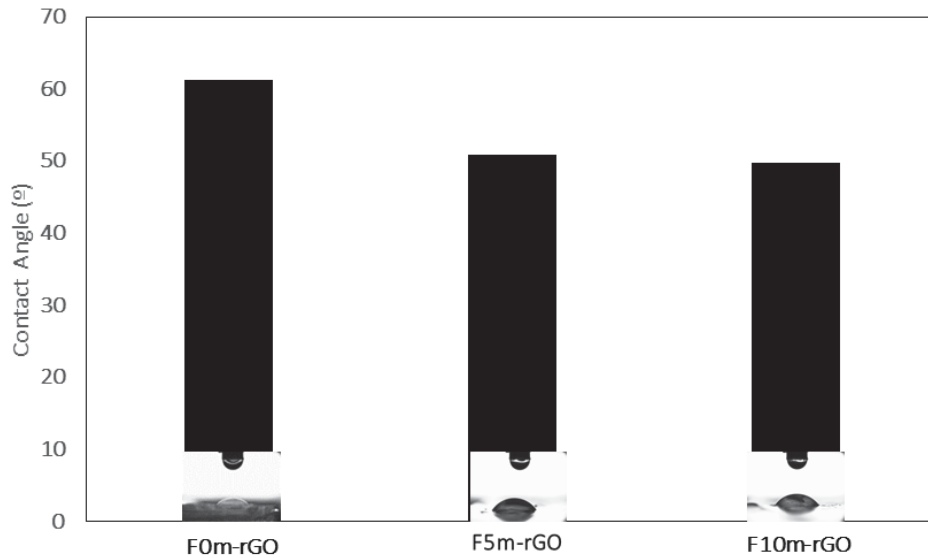

Figure 5: Contact angles of coatings

4.5 Conductivity of screen-printed lines

The electrical conductivity of the screen-printed lines was measured and given in Figure 6. Figure 6 showed that the conductivity of polyurethane acrylate coating is low, 1.82×10^{-17} S/cm, which belongs to insulator. When m-rGO nanoparticles were added, the conductivity increased remarkably. It could be explained that the conductivity results of nano materials. With the increase of the content of m-rGO nanoparticles the contact density between conductive fillers increased, the conductive path became more, and the conductivity increased rapidly. Results are consistent with the literature (Li et al., 2019).
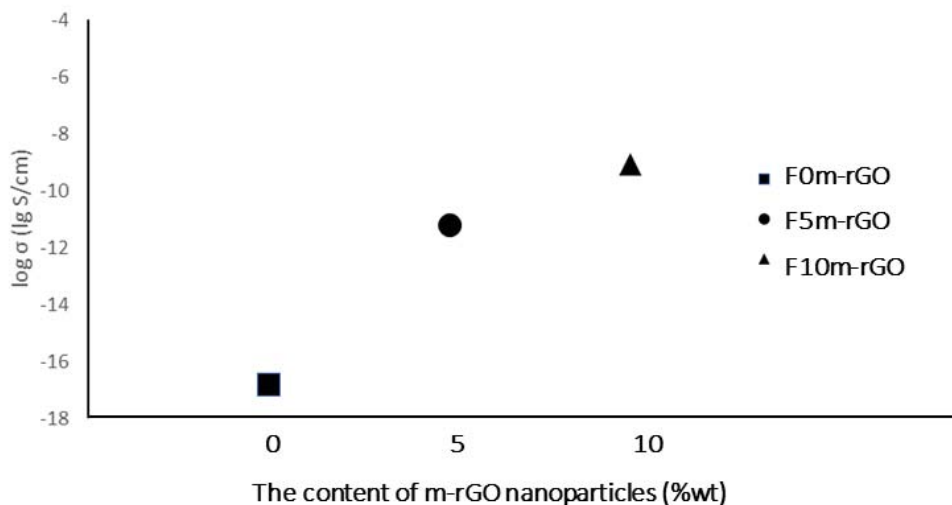

Figure 6: Electrical conductivity m-rGO nanoparticles of added PUA screen printed lines

5. CONCLUSIONS

In summary, surface modified reduced graphene oxide nanoparticles loaded UV curable conductive inks based on PUA chemistry were formulated. A focus was spent on understanding the composition effects on the ink properties that subsequently dictates its screen printability and finally the electrical, thermal and flammibility properties. For this purpose, acr-rGO was prepared and successfully characterized using FTIR, then acr-rGO was reacted with DOPO and surface modified r-GO (m-rGO) was obtained. Based on the successful modification reactions, screen-printing ink containing TMPTA, PUA and different amount of m-rGO content (0, 5 and 10 wt%) were prepared. The prepared ink formulations were applied to the paper surface by screen printing (printed coatings). The electrical properties, thermal properties and LOI values increased as expected as the amount of surface modified graphene oxide nanoparticles increased. But the values are not very high, we can attribute this to the low amount of the nanoparticle's additive added. It has been determined that printed conductive paths with the same formulation as coatings with good printability properties balance the insulating structure of PUA towards the conductor. It has been concluded that the obtained ink can be used in printed electronic applications in future studies.

6. REFERENCES

Arman-Kandirmaz, E., Birtane, H., Beyler-Cigil, A. & Ozcan, A. (2020) pH-controlled lavender oil capsulation with ABA-type block copolymer and usage in paper coating. *Flavour and fragrance journal*. 35 (2), 174 - 181. Available from: doi:10.1002/ffj.3549

Burk, L., Gliem, M., Lais, F., Nutz, F., Retsch, M. & Mülhaupt, R. (2018) Mechanochemically Carboxylated Multilayer Graphene for Carbon/ABS Composites with Improved Thermal Conductivity. *Polymers*. 10, 1088. Available from: doi: 10.3390/polym10101088

Cao, J. & Wang, C. (2017) Multifunctional surface modification of silk fabric via graphene oxide repeatedly coating and chemical reduction method. *Applied Surface Science*. 405, 380 - 388. Available from: doi:10.1016/j.apsusc.2017.02.017

Cao, R., Pu, X., Du, X., Yang, W., Wang, J., Guo, H., Zhao, S., Yuan, Z., Zhang, C., Li, C. & Wang, Z.L. (2018) Screen-Printed Washable Electronic Textiles as Self-Powered Touch/Gesture Tribo-Sensors for Intelligent Human–Machine Interaction. *ACS Nano*. 12, 5190 – 5196. Available from: doi:10.1021/acsnano.8b02477

Chen, M.-J., Xu, Y.-J., Rao, W.-H., Huang, J.-Q., Wang, X.-L., Chen, L. & Wang, Y.-Z. (2014) Influence of valence and structure of phosphorus-containing melamine salts on the decomposition and fire behaviors of flexible polyurethane foams. *Industrial & Engineering Chemistry Research*. 53, 8773 – 8783. Available from: doi:10.1021/ie500691p

Chiolerio, A., Bocchini, S., Scaravaggi, F., Porro, S., Perrone, D., Beretta, D., Caironi, M. & Pirri, C. F. (2015) Synthesis of polyaniline-based inks for inkjet printed devices: electrical characterization highlighting the effect of primary and secondary doping. *Semiconductor Science and Technology*. 30, 104001. Available from: doi:10.1088/0268-1242/30/10/104001

Cronin, H. M., Stoeva, Z., Brown, M., Shkunov, M. & Silva, S. R. P. (2018) Photonic Curing of Low-Cost Aqueous Silver Flake Inks for Printed Conductors with Increased Yield. *ACS Applied Materials & Interfaces.* 10, 21398 - 21410. Available from: doi: 10.1021/acsami.8b04157

Faddoul, R., Reverdy-Bruas, N. & Blayo, A. (2012) Formulation and screen printing of water based conductive flake silver pastes onto green ceramic tapes for electronic applications. *Materials Science and Engineering: B*. 177 (13), 1053 – 1066. Available from: doi:10.1016/j.mseb.2012.05.015

Garlapati, S. K., Divya, M., Breitung, B., Kruk, R., Hahn, H. & Dasgupta, S. (2018) Printed Electronics Based on Inorganic Semiconductors: From Processes and Materials to Devices. *Advanced Materials*. 30, 1707600. Available from: doi:10.1002/adma.201707600

Gengenbach, U., Ungerer, M., Koker, L., Reichert, K.-M., Stiller, P., Allgeier, S., Köhler, B., Zhu, X., Huang, C. & Hagenmeyer, V. (2020) Automated fabrication of hybrid printed electronic circuits. *Mechatronics.* 70, 102403. Available from: doi:10.1016/j.mechatronics.2020.102403

He, P., Cao, J., Ding, H., Liu, C., Neilson, J., Li, Z., Kinloch, I. A. & Derby, B. (2019) Screen-Printing of a Highly Conductive Graphene Ink for Flexible Printed Electronics. *ACS Applied Materials & Interfaces*. 11 (35), 32225 – 32234. Available from: doi:10.1021/acsami.9b04589

Hines, D. R., Gu Y., Martin, A. A., Li, P., Fleischer, J., Clough-Paez, A., Stackhouse, G., Dasgupta, A. & Das, S. (2021) Considerations of aerosol-jet printing for the fabrication of printed hybrid electronic circuits. *Additive Manufacturing.* 47, 102325. Available from: doi:10.1016/j.addma.2021.102325

Hong, H., Jiang, L., Tu, H., Hu, J., Moon, K.-S., Yan, X. & Wong C.-P. (2022) Rational design and evaluation of UV curable nano-silver ink applied in highly conductive textile-based electrodes and flexible silver-zinc batteries. *Journal of Materials Science & Technology*. 101, 294 - 307. Available from: doi:10.1016/j.jmst.2021.04.061

Htwe, Y. Z. N. & Mariatti, M. (2022) Printed graphene and hybrid conductive inks for flexible, stretchable, and wearable electronics: Progress, opportunities, and challenges. *Journal of Science: Advanced Materials and Devices.* 7 (2), 100435. Available from: doi:10.1016/j.jsamd.2022.100435

Huang, J., Wu, Y., Cong, J., Luo, J. & Liu, X. (2018) Selective and sensitive glycoprotein detection via a biomimetic electrochemical sensor based on surface molecular imprinting and boronate-modified reduced graphene oxide. *Sensors and Actuators B: Chemical*. 259, 1 – 9. Available from: doi:10.1016/j.snb.2017.12.049

Hyun, W. J., Secor, E. B., Hersam, M. C., Frisbie, C. D. & Francis, L. F. (2015) High-Resolution Patterning of Graphene by Screen Printing with a Silicon Stencil for Highly Flexible Printed Electronics. *Advanced Materials.* 27, 109 – 115. Available from: doi:10.1002/adma.201404133

Joseph, A. M., Nagendra, B., Gowd, E. B. & Surendran, K. P. (2016) Screen-Printable Electronic Ink of Ultrathin Boron Nitride Nanosheets. *ACS Omega*. 1 (6), 1220 – 1228. Available from: doi:10.1021/acsomega.6b00242

Kashiwagi, T., Du, F., Douglas, J. F., Winey, K. I., Harris, R. H. & Shields, J. R. (2005) Nanoparticle networks reduce the flammability of polymer nanocomposites. *Nature Materials*. 4, 928 – 933. Available from: doi:10.1038/nmat1502

Kell, A. J., Paquet, C., Mozenson, O., Djavani-Tabrizi, I., Deore, B., Liu, X., Lopinski, G. P., James, R., Hettak, K., Shaker, J., Momciu, A., Ferrigno, J., Ferrand, O., Hu, J. X., Lafreniere, S. & Malenfant, R. L. (2017) Versatile Molecular Silver Ink Platform for Printed Flexible Electronics. *ACS Applied Materials & Interface.* 9 (20), 17226 – 17237. Available from: doi:10.1021/acsami.7b02573

Li, X., Wang, S., Xie, J., Hu, J. & Fu, H. (2019) Polyurethane acrylate-supported rGO/TiO2 electrical conductive and antibacterial nanocomposites. *International Journal of Polymeric Materials and Polymeric Biomaterials*. 68 (6), 319 - 327. Available from: doi:10.1080/00914037.2018.1452227

Liang, J., Tong, K. & Pei, Q. (2016) A Water-Based Silver-Nanowire Screen-Print Ink for the Fabrication of Stretchable Conductors and Wearable Thin-Film Transistors. *Advanced Materials*. 28, 5986 – 5996. Available from: doi:10.1002/adma.201600772

Lin, C. H., Wu, C. Y. & Wang, C. S. (2020) Synthesis and properties of phosphorus-containing advanced epoxy resins. *Journal of Applied Polymer Science*. 78, 228 – 235. Available from: doi:10.1002/1097-4628(20001003)78:1<228::AID-APP270>3.0.CO;2-Z

Liu, F. & Liu, G. (2018) Enhancement of UV-aging resistance of UV-curable polyurethane acrylate coatings via incorporation of hindered amine light stabilizers-functionalized TiO2-SiO2 nanoparticles. *Journal of Polymer Research*. 25 (2), 1 - 14. Available from: doi:10.1007/s10965-018-1466-x

Liu, G., Chen, W. & Yu, J. (2010) A novel process to prepare ammonium polyphosphate with crystalline Form II and its comparison with melamine polyphosphate. *Industrial & Engineering Chemistry Research*. 49, 12148 – 12155. Available from: doi:10.1021/ie1014102

Ma, Y., Gong, X., Liao, C., Geng, X., Wang, C. & Chu, F. (2018) Preparation and Characterization of DOPO-ITA Modified Ethyl Cellulose and Its Application in Phenolic Foams. *Polymers*. 10, 1049. Available from: doi:10.3390/polym10101049

Mendes-Felipe, C., Oliveira, J., Etxebarria, I., Vilas-Vilela, J. L. & Lanceros-Mendez, S. (2019) State-of-the-Art and Future Challenges of UV Curable Polymer-Based Smart Materials for Printing Technologies. *Advanced Materials Technologies*. 4 (3), 1800618. Available from: doi:10.1002/admt.201800618

Ozcan, A., Kašikovic, N., Arman Kandirmaz, E., Djurdevic, S. & Petrovic, S. (2020) Highly flame retardant photocured paper coatings and printability behavior. *Polymers for Advanced Technologies*. 31 (11), 2647 - 2658. Available from: doi:10.1002/pat.4991

Perelaer, J., Klokkenburg, M., Hendriks, C. E. & Schubert U. S. (2009) Microwave Flash Sintering of Inkjet-Printed Silver Tracks on Polymer Substrates. *Advanced Materials*. 21 (47), 4830 - 4834. Available from: doi:10.1002/adma.200901081

Saengchairat, N., Tran, T. & Chua, C.-K. (2016) A review: additive manufacturing for active electronic components. *Virtual and Physical Prototyping.* 12, 31 - 46. Available from: doi:10.1080/17452759.2016.1253181

Saleh, E., Woolliams, P., Clarke, B., Gregory, A., Greedy, S., Smartt, C., Wildman, R., Ashcroft, I. Hague, R., Dickens, P. & Tuck, C. (2017) 3D inkjet-printed UV-curable inks for multi-functional electromagnetic applications. *Additive Manufacturing*. 13, 143 − 148. Available from: doi:10.1016/j.addma.2016.10.002

Song, P., Liu, H., Shen, Y., Du, B., Fang, Z. & Wu, Y. (2009) Fabrication of dendrimer-like fullerene (C60)-decorated oligomeric intumescent flame retardant for reducing the thermal oxidation and flammability of polypropylene nanocomposites. *Journal of Materials Chemistry A*. 19, 1305. Available from: doi:10.1039/b815610g

Sreenilayam, S. P., Ahad, I. U., Nicolosi, V. & Brabazon, D. (2021) MXene materials based printed flexible devices for healthcare, biomedical and energy storage applications. *Materials Today*. 43, 99 - 131. Available from: doi:10.1016/j.mattod.2020.10.025

Tissera, N. D., Wijesena, R. N., Perera, J. R., de Silva, K. N. & Amaratunge, G. A. (2015) Hydrophobic cotton textile surfaces using an amphiphilic graphene oxide (GO) coating. *Applied Surface Science*. 324, 455 - 463. Available from: doi:10.1016/j.apsusc.2014.10.148

Verboven, I. & Deferme, W. (2021) Printing of flexible light emitting devices: A review on different technologies and devices, printing technologies and state-of-the-art applications and future prospects. *Progress in Materials Science*. 118, 100760. Available from: doi:10.1016/j.pmatsci.2020.100760

Wu, W. (2017) Inorganic nanomaterials for printed electronics: a review. *Nanoscale*. 9, 7342 - 7372. Available from: doi:10.1039/C7NR01604B

Zhang, X., Wang, X., Lei, Z., Wang, L., Tian, M., Zhu, S., Xiao, H., Tang, X. & Qu, L. (2020) Flexible MXene-Decorated Fabric with Interwoven Conductive Networks for Integrated Joule Heating, Electromagnetic Interference Shielding, and Strain Sensing Performances. *ACS Applied Materials & Interfaces.* 12, 14459 - 14467. Available from: doi:10.1021/acsami.0c01182